Fusion Engineering and Design 89 (2014) 1151–1157

Contents lists available at ScienceDirect

Fusion Engineering and Design

journal homepage: www.elsevier.com/locate/fusengdes

A discrete element method study on the evolution of thermomechanics of a pebble bed experiencing pebble failure

Jon T. Van Lew*, Alice Ying, Mohamed Abdou

UCLA, MAE Department, 44-114 Engineering IV, 420 Westwood Plaza, Los Angeles, CA 90095-1597, USA

ARTICLE INFO

Article history:
Received 30 September 2013
Received in revised form 9 April 2014
Accepted 23 April 2014
Available online 2 June 2014

Keywords:
Pebble bed thermomechanics
DEM
Discrete element method
Pebble failure
Effective thermal conductivity

ABSTRACT

The discrete element method (DEM) is used to study the thermal effects of pebble failure in an ensemble of lithium ceramic spheres. Some pebbles crushing in a large system is unavoidable and this study provides correlations between the extent of pebble failure and the reduction in effective thermal conductivity of the bed. In the model, we homogeneously induced failure and applied nuclear heating until dynamic and thermal steady-state. Conduction between pebbles and from pebbles to the boundary is the only mode of heat transfer presently modeled. The effective thermal conductivity was found to decrease rapidly as a function of the percent of failed pebbles in the bed. It was found that the dominant contributor to the reduction was the drop in inter-particle forces as pebbles fail; implying the extent of failure induced may not occur in real pebble beds. The results are meant to assist designers in the fusion energy community who are planning to use packed beds of ceramic pebbles. The evolution away from experimentally measured thermomechanical properties as pebbles fail is necessary for proper operation of fusion reactors.

1. Introduction

Lithiated ceramic pebbles have been chosen by many participants in ITER experiments as a material to be used for tritium generation [1–4]. Adjustments in the manufacturing processes of the ceramic pebbles permits variation of characteristics such as the pebble's tritium retention and release properties, lithium density, opened- and closed-porosity, nominal diameter, and crush strength. The variations are often coupled. For instance, for the sake of tritium management the open porosity is often increased which comes at the expensive of a decreased crush strength of the pebble. Because of the relatively weak crush strength distributions among batches of pebbles as well as the value of stresses predicted in the pebble bed, it is inevitable that during operation in the fusion environment individual pebbles will 'fail' in the ensemble. Designers of lithium ceramic tritium breeding blankets must mitigate pebble failure but also anticipate the breadth and magnitude of effects that some unavoidable failure will have on macroscopic properties.

To develop a complete numerical model for a pebble bed requires completing many interactive sub-models. To demonstrate, we give here the path of a possible analysis scheme of these models. To begin, one must have knowledge of the interaction of the pebble bed with the containing structure as they exist in a fusion environment. The interactions are generally analyzed via the finite element method to find internal stresses and temperature fields of the entirety of the pebble bed. After the internal fields are mapped, one would use the discrete element method (DEM) to interpret the macro-scopic stress fields into the inter-particle forces. With the inter-particle forces and total absorbed thermal energy calculated, a prediction of the initiation of pebble failure would predict the number of pebbles (if any) that would be crushed in that computational volume. When a pebble is crushed, it loses contact with its neighbors and subsequently breaks any thermal or mechanical transport that the pebble was providing. Fragmentation of a failed pebble would also be handled by the DEM with another model. Following this, DEM would determine how the pebble bed re-settles and effective properties evolve in the presence of failed pebbles. Finally, the updated bed properties would feed back into the FEM formulation to predict how overall stress fields and material interactions are altered in light of the failure. The fusion community is far from an integrated simulation that can follow such a path, but it is the principle goal of the overall efforts at UCLA.

Research on pebble failure up to now has focused on predicting when pebbles may fail in a bed as a function of an external load (typically, stress from walls). In this study, we analyze the evolution of pebble bed properties assuming some fraction of pebbles

* Corresponding author. Tel.: +1 5209093238.
E-mail address: jtvanlew@fusion.ucla.edu (J.T. Van Lew).

http://dx.doi.org/10.1016/j.fusengdes.2014.04.066
0920-3796/

in the ensemble have failed. The focus of this study is to determine the extent of change in aggregate ensemble properties due to individual pebble failure, as well as help designers anticipate acceptable limits of pebble failure from a thermal-management point of view. We make use of DEM to simulate individual pebbles in a packed bed. From this scale of simulation, we can study single pebbles undergoing failure while the bed as a whole is subject to mechanical and thermal boundaries.

For the DEM tools used in this study, the only mode of heat transfer is conduction through the solids. In a fusion breeder however, the helium purge gas winding through the interstitial gaps of the pebbles will have a large contribution to overall heat transfer [5,6]. To overcome the current limit on DEM heat transfer, we are also working with computational fluid dynamics coupling to the discrete element method to account for the helium energy transport. The next step is to combine our analysis tools with a failure initiation predictor as well as a new method of simulating a pebble after failure. Those modeling enhancements will be reported in the future. As these models become more comprehensive in their scope, the fusion community will be better prepared to determine the survivability and performance of a solid breeder design in the fusion environment.

2. Pebble failure modeling

The discrete element method has been used for studies in a variety of fields for studying inter-particle forces and the homogeneously distributed force networks that arise in packed beds (for example, see Ref. [7]). The discrete element method was also used in the fusion community to attempt to model failure initiation and propagation [8–10]. They too observed that a relatively few number of high-force networks, distributed throughout the bed supported the external mechanical loads. The even distribution of the force networks was used to defend the development of a probability-based predictor for failure. We make use of the probability argument of Zhao et al. for the current study [10]. Their basic premise is that probability distributions of strength curves for pebble crushing have been observed (see, for example crush loads of Ref. [3]). Then in DEM models, a probability distribution of inter-particle forces are also observed. Overlaying the two probabilities resulted in seemingly random locations of pebbles satisfying the failure criteria – not strictly along the high-force chains running through packed beds.

We apply the theory of Zhao et al. in the following manner. If pebbles fail at random locations, we may de-couple the task of predicting pebble failure (*i.e.* finding the mechanical or thermal load that causes a pebble to fail) from the task of modeling the ramifications of pebble failure. In our model, we begin with a starting point of a packed bed and then simply flag pebbles at random for 'failing'. For our first model of failure, after a pebble has been flagged it is removed from the system entirely. The removal disrupts the metastatic state of the ensemble and the remaining pebbles re-settle. In reality, the ceramic pebbles generally break into just a few large pieces that remain in the system. Under development is a method for recreating that behavior in the DEM domain, it will be reported in future studies.

Our three-dimensional system consists of mono-dispersed particles of diameter d. The particles are constrained by two rigid walls in the x-direction at locations of $x = \pm 10d$ and periodic boundary conditions in the y-direction located at $y = \pm 7.5d$. Gravity acts in the downward z-direction and the particles are bound from below by a rigid wall at $z = 0$. The size of the system allows approximately 10 000 particles to fill to a height of approximately $z = 30d$. The volume was chosen to represent the long, tall, narrow channels seen in many solid breeder module designs [11–13].

2.1. Particle dynamics

To summarize the discrete element method, we consider a Lagrangian approach to particle tracking. Every particle in the system is followed through time with position, velocity, and acceleration values that are derived from interactions with neighboring particles and gravity. To demonstrate a force calculation between pebbles, imagine two particles, labeled i and j, located at $\mathbf{r}_i$ and $\mathbf{r}_j$, respectively. The pebbles are allowed to virtually overlap at a distance we can find as $\delta = (R_i + R_j) - |\mathbf{r}_i - \mathbf{r}_j|$.

The forces of overlapping, elastic spheres are then found directly via Hertz–Mindlin theory. The equations are described in great detail in papers such as Refs. [14,15]. Here we give only a summary of some pertinent equations. The motion of particle i is governed by the following force balance

$$F_i = m_i g + \sum_j^Z (k_n \delta_{n_{ij}} - \gamma_n v_{n_{ij}}) + (k_t \delta_{t_{ij}} - \gamma_t v_{t_{ij}}) \quad (1)$$

where m is the mass, g is gravity, and Z is the coordination number (*i.e.* number of contacting neighbors), and $v_{n/t}$ is the normal/tangential velocity, respectively. The spring-dashpot constants, from [14–16], are

$$k_n = \frac{4}{3} E^* \sqrt{R^* \delta_{n_{ij}}} \qquad \gamma_n = -2\sqrt{\frac{5}{6}} \beta \sqrt{S_n m^*}$$

$$k_t = 8 G^* \sqrt{R^* \delta_{t_{ij}}} \qquad \gamma_t = -2\sqrt{\frac{5}{6}} \beta \sqrt{S_t m^*}$$

In Hertz–Mindlin formulations $S_n = (3/2)k_n$, $S_t = k_t$, and β is a function of the coefficient of restitution, ϵ, $\beta = \ln \epsilon / \sqrt{\ln^2 \epsilon + \pi^2}$.

Owing to the impact thermal expansion has on pebble bed structures undergoing thermal cycling [17–19], we also included a simple thermal expansion model. The diameter of the pebbles was updated after a specific number of timesteps according to the following

$$d_i = d_{0,i}[1 + \alpha(T_i - T_{\text{ref}})] \quad (2)$$

where α is the thermal expansion coefficient, T_i is the temperature of the pebble at the current step, and $d_{0,i}$ is the diameter of the pebble at temperature T_{ref}.

We note that the spring-dashpot constants do not need empirical fitting functions but are instead determined completely from material and geometric properties: Young's Modulus, E^*, shear modulus, G^*, pair mass, m^*, and relative curvature, R^*. And their interactions, of Eq. (1), are easily derived from first principles. The definitions of these effective properties, $[]^*$, are given in Appendix A.

Time-discretization of the integration of Eq. (1) is handled by the core Large-scale Atomic/Molecular Massively Parallel Simulator (LAMMPS) code released by Sandia National Laboratories [20,21]. The code calculates velocity and position via the semi-explicit velocity-Verlet integration. The algorithm is stable with a global error of approximately $O(\Delta t^2)$ for displacement; details can be found in Ref. [22].

In the process of the study, to demonstrate the ability of the dynamic integration to capture resettling (and any possibly asymmetries), some beds were generated wherein the failure of pebbles was slightly localized near one or both x-walls. The profile of the pebbles near the top of the stack, after resettling, are shown in Fig. 1.

In our work, we occasionally required a fully quiesced bed. To determine when this occurred, the total kinetic energy of the entire ensemble was monitored and a packed bed was considered to have completely settled once the kinetic energy of the system was less than 10^{-9}; similar to the process described in Ref. [23].

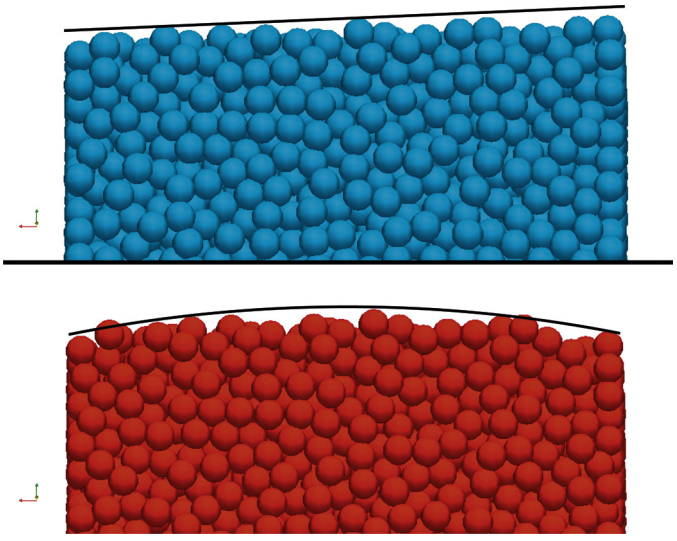

Fig. 1. Demonstrating the dynamic resettling from an example study done on location bias to pebble failure. The top image had the pebbles near the left wall biased to fail. The bottom image had a bias for the pebbles near both walls to fail. The lines are drawn as an aid to the eye.

2.2. Granular heat conduction

Handling the heat transfer between contacting particles has been investigated extensively by researchers in a number of fields and we apply their theory here [24–29]. In this study, we have begun by considering only conduction between particles. In such a situation, the amount of energy per time that can be transported per difference in temperature between pebble i and j is given by Batchelor and O'Brien [30] as a conductance h_{ij}. Defined as

$$\frac{h_{ij}}{k^*} = 2a = 2\left[\frac{3F_nR^*}{4E^*}\right]^{1/3} \tag{3}$$

where a is the contact radius of two overlapping spheres, $k^* = 2k_ik_j/(k_i + k_j)$ is the effective solid conductivity of the two particles, and F_n is the magnitude of the normal force between particles i and j. Therefore, if we consider particles at temperatures T_i and T_j in contact, they will transfer heat at a rate of

$$Q_{ij} = h_{ij}(T_i - T_j) \tag{4}$$

The temperature of a single pebble is found from the first law of thermodynamics

$$\rho_i V_i C_i \frac{dT_i}{dt} = Q_{s,i} + \sum_j^Z Q_{ij} \tag{5}$$

where ρ is the pebble density, V is the volume of the pebble, C is the specific heat of the pebble, and we sum heat conducted over all neighboring contacts. The energy equation also allows for nuclear heating of the pebble with Q_s. In the model, the physical walls in the x-plane behave as temperature reservoirs that we specify. The pebbles that are in contact with the wall conduct heat into the reservoir with the same mechanisms as particle–particle heat transfer.

Implicit in the energy balance equation is the fact that a lumped capacitance method is being assumed for every pebble. Additionally, we are assuming that in a single timestep a pebble is transferring heat only with its immediate neighbors. Vargas and Mccarthy [27] provide arguments for the validity of Eq. (5) given numeric time steps and contact areas. The conclusion is that any time step that satisfies stability of the particle dynamics will automatically satisfy particle heat transfer.

Table 1
Maximum load and nominal tension.

E (GPa)	ν	k (W/m K)	C (J/kg K)	α (1/K)
126	0.24	2.5	1156	15×10^{-6}

Because of the chosen geometry of the pebble beds under analysis here, the heat transfer is essentially one-dimensional through the x-direction. The pebble bed has very little variation of forces and temperatures in the y-direction due to the periodic boundary condition at the edges of the domain. Gravity effects are minor in the overall heat transfer and induce only a slight z-dependency to the results; negligibly so in nearly all our simulations. With the one-dimensional assumption, we step back into a continuum mechanics formulation and find an effective thermal conductivity of a steady-state pebble bed. A steady state for a material with constant temperature boundary conditions ($T(\pm 10d) = T_s$) and nuclear heating has the following heat equation

$$0 = \frac{d^2T}{dx^2} + \frac{q'''}{k_{\text{eff}}} \tag{6}$$

where in our case the volumetric heating term, $q''' = Q_{\text{tot}}/V_{\text{tot}} = (Q_sN)/(300Hd^2)$; where H is the average height of the top layer of pebbles. We apply symmetry about the centerline and impose our boundary conditions to solve the differential equation. If we take the temperature of the midplane as $T(0) = T_0$, we back-out an effective thermal conductivity (ETC) as

$$k_{\text{eff}} = \frac{Q_sN}{6H(T_0 - T_s)} \tag{7}$$

We will use this formulation to analyze and compare our test-case pebble beds.

The granular heat transfer equations (Eqs. (3)–(5)) are layered onto the LAMMPS code via a package of code named LIGGGHTS (LAMMPS Improved for General Granular and Granular Heat Transfer Simulations [31]). Parallelization of the code is straightforward with LAMMPS and we run the code on 128 nodes of UCLA's Hoffman2 cluster for typical run times of 18–24 h per routine (*e.g.* filling, packing, heating, etc.).

2.3. Material properties

For this study, the material was chosen as lithium metatinatate with all properties coming from Ref. [32]; they are summarized in Table 1.

2.4. Methodology

All the test cases begin with a common starting point of a filled, lightly packed volume of 10 550 pebbles. The pebbles are poured into the volume from above and come to rest under the influence of gravity (see Fig. 2). Initially, to recreate how we may pack solid breeders in reality, we attempted vibration simulations in order to pack the pebbles into a more dense state. However, we found the same packing states (from a void fraction standpoint) could be realized in a more computationally-simple manner by lowering a z-plane wall onto the top of the packed bed until it experienced some small force. This pour-press-packing routine was repeated many times and all the beds exhibited the same force on the top wall at roughly the same packing fraction. We took the last case, with a packing fraction (volume of N pebbles per total volume) of $\phi_{\text{bl}} = 62.9\%$, as our baseline configuration. The packed bed state was saved and used as a starting point for numerous 'failed' cases to be described later.

For the baseline case, we assigned an initial temperature of T_{ref} to both the pebbles and the x walls, then set a constant nuclear

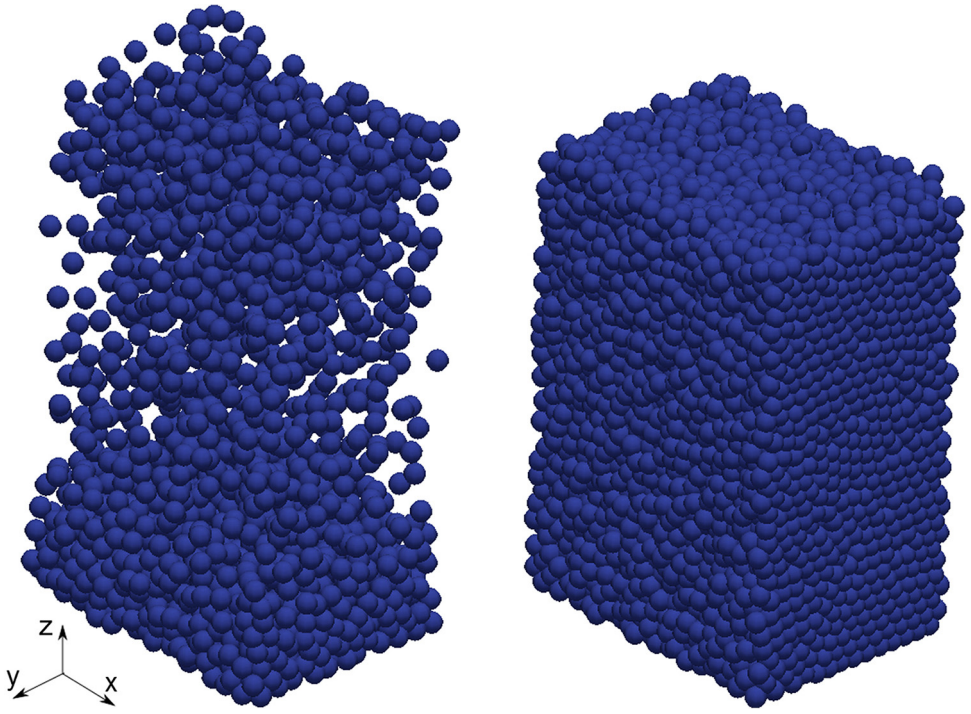

Fig. 2. Demonstrating the pouring process of $N = 10\,550$ pebbles into the control volume with an early (left) and late (right) snapshot.

heating source on each pebble. The nuclear energy raised the temperature of the pebbles while the walls remained at T_{ref} for cooling. The process ran until a steady state was reached (for example, see Fig. 3); the total thermal energy of the bed, $E = \sum_i^N m_i C_i T_i$, was monitored and the simulation completed when the value was constant. At steady state, we analyzed thermomechanical characteristics of the pebble bed such as effective thermal conductivity, average coordination number, temperature profiles in the bed, and inter-particle contact forces.

As mentioned in Section 2, in this study we model pebble failure without considering the cause of failure. This is done by randomly selecting pebbles from the ensemble, regardless of forces acting upon the pebble, and removing them entirely. When a pebble is removed, the neighboring pebbles react due to the imbalance of forces and the bed settles into a new configuration. We differentiated the failed beds by their percentage of failed pebbles: η = number of failed pebbles per original ensemble size. After failing we again applied our heating routine.

3. Results and discussions

The aim of this study was both to discover the impact of pebble failure on thermomechanical properties as well as determine the impact as a function of the number of failed pebbles. To satisfy the latter, we created beds with $\eta = 1\%$, 5%, 10%, and 15% of pebbles failed.

We first compare steady-state temperature profiles in the test beds against the one-dimensional theory of Eq. (6). To find the temperature profile in x, we create volumes of width Δx that extend through the limits of the y- and z-directions. We then find the n pebbles residing in the slices and take the mean value of their temperatures, $\langle T \rangle = \sum_i^n T_i/n$ of all pebble temperatures that have coordinates inside the slice. Below we will omit the notation $\langle T \rangle$ with the understanding that temperatures are volume-averages. Using the volume slices, we also find the average

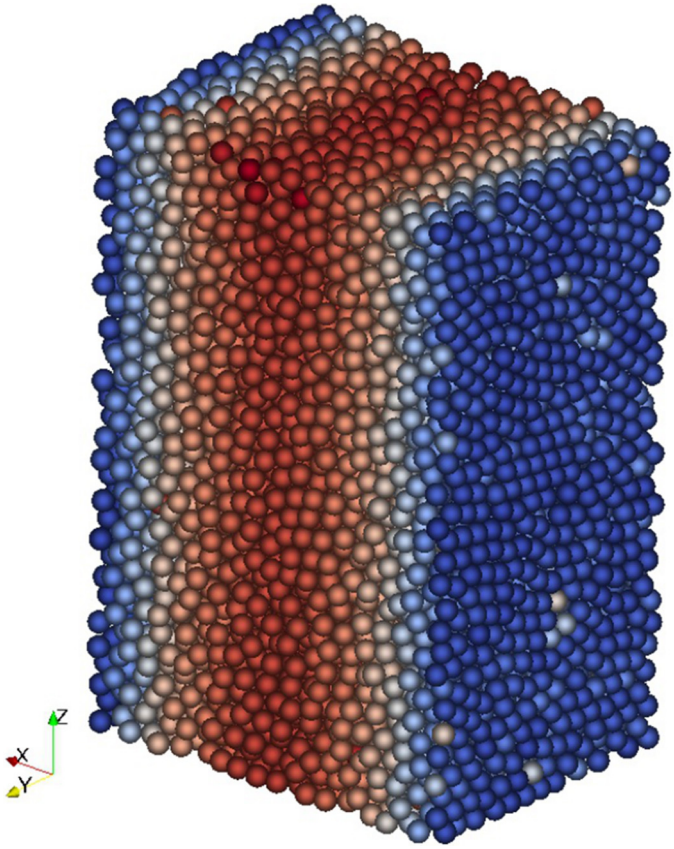

Fig. 3. Temperature distribution of pebbles in the 10% failed bed. At the end of steady-state heating, a one-dimensional profile is evident in all pebble beds studied here. The pebbles are receiving nuclear heating. Cooling proceeds through the pebbles in contact with the walls in the x-direction.

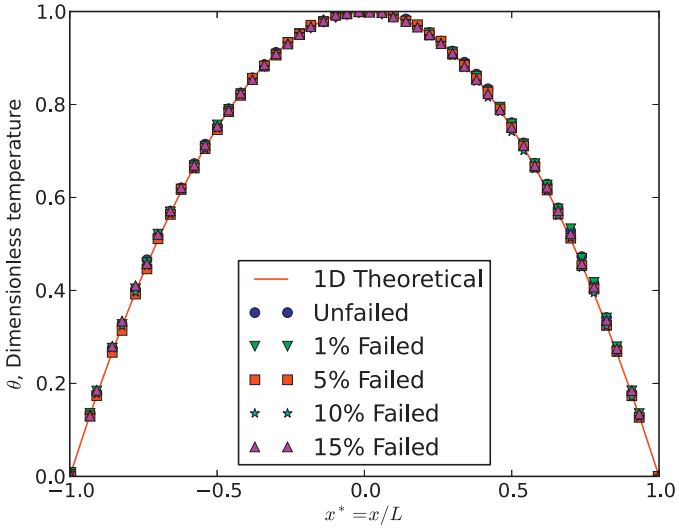

Fig. 4. The non-dimensional temperature profiles for each test case follow the theoretical shape of a one-dimensional, constant k, continuum solution.

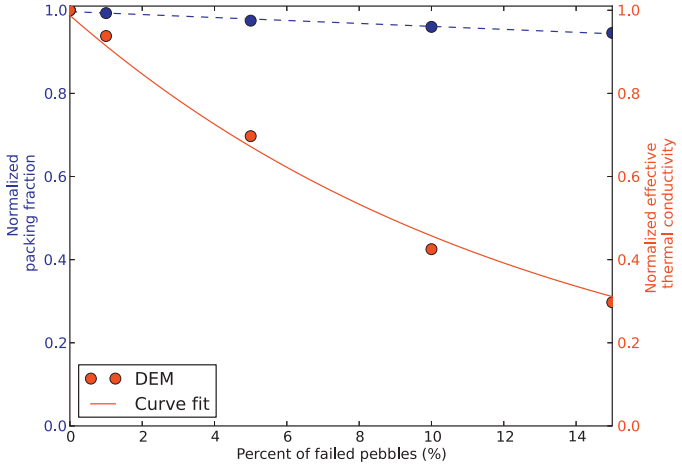

Fig. 5. The normalized effective thermal conductivity (solid line) follows an exponential decay relationship with amount of failed pebbles. The normalized packing fraction (dashed line), compared to thermal conductivity, is relatively constant and is more closely fit to a linear reduction.

coordination number, $\langle Z\rangle = \sum_i^n Z_i/n$, normalized average contact force, $\langle F^*\rangle = [\langle F\rangle/\langle F_{\text{bl}}\rangle_{\max}]^{1/3}$, and the normalized average temperature difference between pebbles in the slice, $\langle \Delta T_{ij}\rangle/(T_0 - T_s)_{\text{bl}}$; parameters which are discussed later.

When analytically solving Eq. (5), we introduce non-dimensional temperature, $\theta_{1\text{D}} = (T - T_s)/(T_0 - T_s)$, and spatial, $x^* = x/L$, variables and the solution becomes purely geometric; $\theta_{1\text{D}} = 1 - x^{*2}$. We plot this theoretical solution against the temperature profiles coming from the steady-state DEM simulation in Fig. 4. We find that all our models had a nearly perfect match to a one-dimensional prediction, validating the calculation of effective thermal conductivity in this study.

Another concern we had for pebble failure, was the phenomenon of 'jamming' during resettling that would possibly leave pebbles isolated from their neighbors (apart from those they are resting upon). Such an isolated pebble would have no strong pathway for heat transfer and heat up much higher than that of its neighbors. Evidence of pebble isolation and 'hot-spots' would be apparent in Fig. 4 as localized deviations of data points from the quadratic profile. However, no deviations are seen in the data and we conclude that hot-spots will not be a concern in a packed bed.

The effective thermal conductivity is found for all of our pebble beds, via Eq. (7), then normalized against the conductivity of the baseline ensemble ($k^*_{\text{eff}} = k_{\text{failed}}/k_{\text{bl}}$). Fig. 5 shows the decreasing ETC with pebble failure. When 15% of the pebbles are crushed in a pebble bed, the ETC has fallen all the way to only $k^*_{\text{eff}} = 0.30$. This large reduction is especially important in light of the already poor thermal management of virgin pebble beds that, even in helium environments, have been experimentally measured at only approximately 1 W/m K (see, *e.g.*, Refs. [5,33]). In well-packed pebble beds, the ETC is generally related to the packing fraction. In Fig. 5, this relationship seems weak as the effective conductivity drops much more rapidly than does the packing fraction as the number of broken pebbles in the ensemble increases. To find the cause of decrease in conductivity and to make use of the information provided by DEM tools, we look to other parameters than the packing fraction.

From Eq. (5), in the steady-state, the energy input by nuclear heating must be balanced by the transport of heat out of a pebble into its neighbors. Inter-particle heat transfer is dictated by the number of neighboring contacts, temperature difference between pebbles, and the thermal conductance, h_{ij} through the contact area. The thermal conductance is, itself, a function of material properties (which are essentially constant here) and the force at the contact, going as $h_{ij} \propto F_n^{1/3}$. Thus, the net heat out is a function of the three variables as

$$Q_{\text{net}} = f(Z, F_n^{1/3}, \Delta T) \tag{8}$$

The variables affecting Q_{net} are plotted in Fig. 6. The average coordination number, shown in the bottom plot, decreases from a mid-line value of about 7.0 at the steady-state of the baseline case down to a mid-line value of 5.5 for the 15% failed bed; a reduction of about 80%. But this number does not compare with the large reduction in ETC which was $k^*_{\text{eff}} = 0.30$. Clearly, there are fewer contacts in the pebble bed after failure but this alone does not account for the reduction in ETC.

Much more dramatic, seen in the center plot, is the reduction in average normal force seen by pebbles after many of the neighbors fail and are removed from the system. From the baseline down to the 15% failed case, the contact forces are dramatically reduced to about $\langle F^*\rangle$=0.1. This reduction in force is joined by an increase in average neighbor temperatures which are 3 times higher for the bed with most failed pebbles when compared to the baseline.

The results shown in Fig. 6 demonstrate that the heat transfer through a pebble bed is simultaneously a function of the coordination number and inter-particle contact forces – which are both reduced as pebbles in the bed fail – as well as the temperature difference between pebbles at steady state – which increases as pebbles in the ensemble fail. Interestingly, when a pebble bed has lower overall inter-particle contact forces fewer particles would be expected to break. This would imply that pebble breakage is self-dampening; as pebbles begin to break the ensemble quickly relaxes and avoids future pebble failure. So while we induced failure up to $\eta = 15\%$, such large values may not occur in real beds.

Another feature of Fig. 6 worth noting is the increase in averaged normal contact forces near the center of the bed relative to the walls. In the assumptions used to develop this simulation, we had noted the lack of localized force concentrations in a bed under an external mechanical load. However, in these results, owing to the nuclear heating temperature profile and thermal expansion of each pebble, there is a bias toward higher forces in the center of the bed. This result highlights the need for a model to predict failure initiation in place of the assumption of random pebble failure.

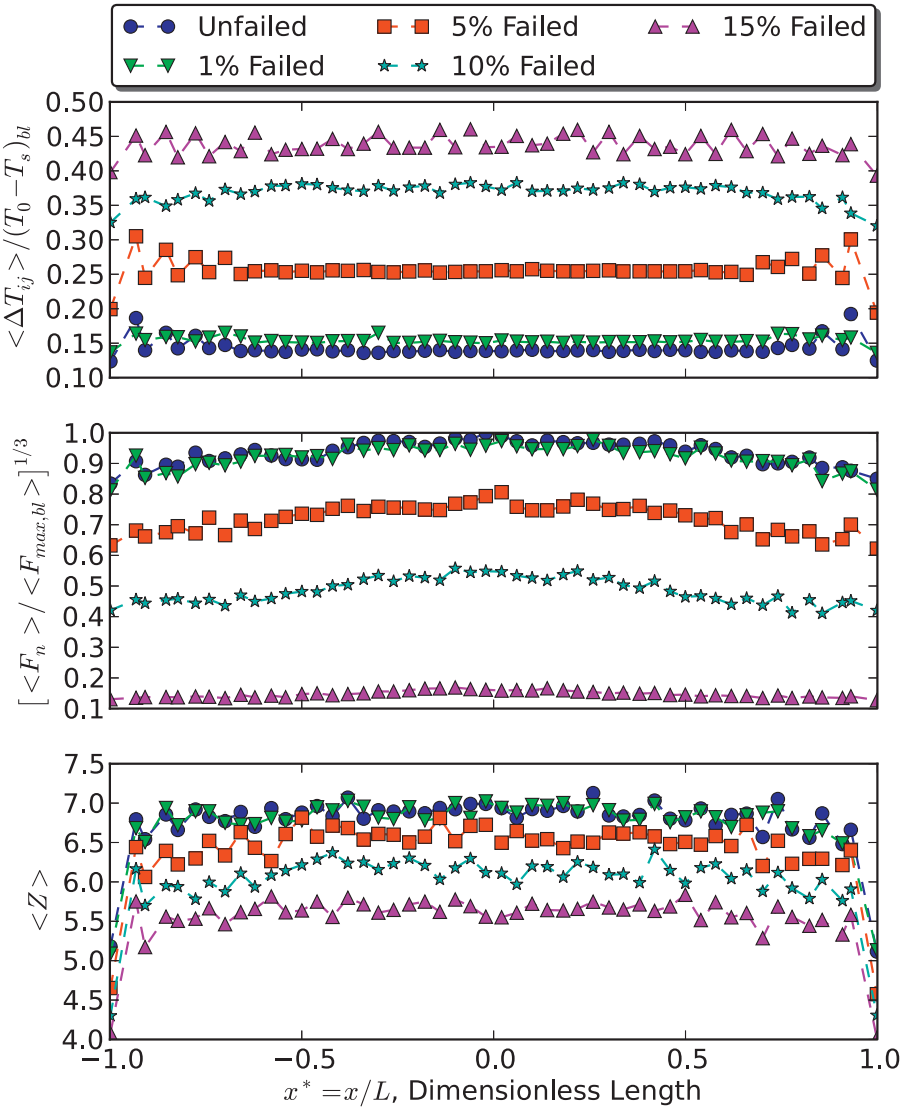

Fig. 6. Average temperature differences between neighboring pebbles (top), contact forces (middle) and coordination numbers (bottom). The profiles of average coordination number and contact forces in the bed decrease in value with increasing pebble failure. Fewer and weaker contacts will reduce the possible paths of heat transfer from a pebble and this results in higher average temperatures between neighbors.

4. Conclusions

The current study aimed at properly simulating a pebble bed with a specified fraction of the pebbles failing during operation; then determining the repercussions of the failures as they affect the macroscopic property of effective thermal conductivity. We used the assumption of homogeneous, random locations of pebble failure to induce a failure routine without requiring external loads on the bed to permit beds that could be directly compared. After heating to a steady-state, an effective thermal conductivity was calculated for the pebble bed. The results show that small amounts of pebble failure correspond to large decreases in the conductive transport of energy through the pebble bed. The increase was due primarily to a drop in the inter-particle forces which lead to a large increase in temperature differences between neighboring pebbles. We note again, however, that this value has been calculated in the absence of interstitial gas so the results apply only to the reduction in energy transferred via inter-particle conduction.

The assumption of homogeneous distribution of pebble failure was found to be inappropriate after a pebble bed reached steady state nuclear heating. The scheme assumes no localization of average forces in the bed but we found an average force profile that had a maximum at the center and minimum at the walls. The next step of modeling will eliminate the error of such an assumption as we must combine failure prediction to failure outcome modeling.

Acknowledgement

This work was performed with support from US Department of Energy, Office of Fusion Energy Sciences, under Grant No. DE-FG02-86ER52123.

Appendix A. Effective material relationships

In the Hertz–Mindlin model, effective material properties are used. These values are based on the two particles interacting. The effective Young's Modulus, E^* is

$$\frac{1}{E^*} = \frac{1-\nu_i^2}{E_i} + \frac{1-\nu_j^2}{E_j}$$

Similarly the effective shear modulus is

$$\frac{1}{G^*} = \frac{2(2+\nu_i)(1-\nu_i)}{E_i} + \frac{2(2+\nu_j)(1-\nu_j)}{E_j}$$

In heat transfer, we also have an effective thermal conductivity of two solid particles. This is

$$k^* = \frac{2k_i k_j}{k_i + k_j}$$

Lastly, the effective radius between two pebbles is

$$\frac{1}{R^*} = \frac{1}{R_i} + \frac{1}{R_j}$$

and likewise the pair mass is

$$\frac{1}{m^*} = \frac{1}{m_i} + \frac{1}{m_j}$$

References

[1] J.D. Lulewicz, N. Roux, Fabrication of Li_2TiO_3 pebbles by the extrusion spheronisation sintering process, J. Nucl. Mater. 311 (2002) 803–806.

[2] D. Mandal, D. Sathiyamoorthy, V.G. Rao, Preparation and characterization of lithium titanate pebbles by solid-state reaction extrusion and spherodization techniques for fusion reactor, Fusion Eng. Des. 87 (January) (2012) 7–12.

[3] K. Tsuchiya, H. Kawamura, K. Fuchinoue, H. Sawada, K. Watarumi, Fabrication development and preliminary characterization of Li_2TiO_3 pebbles by wet process, J. Nucl. Mater. 258–263 (October) (1998) 1985–1990.

[4] S. Cho, M.-Y. Ahn, I.-K. Yu, Y.-H. Park, D.Y. Ku, S.-J. Lee, et al., R&D progress of Korean HCSB TBM, Fusion Eng. Des. 87 (August) (2012) 386–391.

[5] J. Reimann, S. Hermsmeyer, Thermal conductivity of compressed ceramic breeder pebble beds, Fusion Eng. Des. 61–62 (November) (2002) 345–351.

[6] A. Abou-Sena, A.Y. Ying, M.A. Abdou, Effective thermal conductivity of lithium ceramic pebble beds for fusion blankets: a review, Fusion Sci. Technol. 47 (4) (2005) 1094–1100.

[7] H. Makse, D. Johnson, L. Schwartz, Packing of compressible granular materials, Phys. Rev. Lett. 84 (May) (2000) 4160–4163.

[8] R.K. Annabattula, Y. Gan, S. Zhao, M. Kamlah, Mechanics of a crushable pebble assembly using discrete element method, J. Nucl. Mater. 430 (November) (2012) 90–95.

[9] S. Zhao, Y. Gan, M. Kamlah, T. Kennerknecht, R. Rolli, Influence of plate material on the contact strength of Li_4SiO_4 pebbles in crush tests and evaluation of the contact strength in pebble–pebble contact, Eng. Fract. Mech. 100 (2012) 28–37.

[10] S. Zhao, Y. Gan, M. Kamlah, Failure initiation and propagation of Li_4SiO_4 pebbles in fusion blankets, Fusion Eng. Des. 88 (January) (2013) 8–16.

[11] S. Cho, M.-Y. Ahn, D.H. Kim, E.-S. Lee, S. Yun, N.Z. Cho, et al., Current status of design and analysis of Korean Helium-Cooled Solid Breeder Test Blanket Module, Fusion Eng. Des. 83 (December) (2008) 1163–1168.

[12] Y. Poitevin, L. Boccaccini, M. Zmitko, I. Ricapito, J. Salavy, E. Diegele, et al., Tritium breeder blankets design and technologies in Europe: development status of ITER Test Blanket Modules, test & qualification strategy and roadmap towards DEMO, Fusion Eng. Des. 85 (December) (2010) 2340–2347.

[13] M. Enoeda, Y. Kosaku, T. Hatano, T. Kuroda, N. Miki, T. Honma, et al., Design and technology development of solid breeder blanket cooled by supercritical water in Japan, Nucl. Fusion 43 (2003) 1837–1844.

[14] A. Di Renzo, F.P. Di Maio, Comparison of contact-force models for the simulation of collisions in DEM-based granular flow codes, Chem. Eng. Sci. 59 (February) (2004) 525–541.

[15] Y. Tsuji, T. Kawaguchi, T. Tanaka, Discrete particle simulation of two-dimensional fluidized bed, Powder Technol. 77 (October) (1993) 79–87.

[16] N. Brilliantov, F. Spahn, J. Hertzsch, T. Pöschel, Model for collisions in granular gases, Phys. Rev. E: Stat. Phys. Plasmas Fluids Relat. Interdiscip. Topics 53 (May) (1996) 5382–5392.

[17] H. Tanigawa, Y. Tanaka, M. Enoeda, Packing behaviour of a Li_2TiO_3 pebble bed under cyclic loads, J. Nucl. Mater. 417 (December) (2010) 2010–2012.

[18] W.L. Vargas, J.J. Mccarthy, Thermal expansion effects and heat conduction in granular materials, Phys. Rev. E: Stat. Nonlin. Soft Matter Phys. 76 (October) (2007) 1–8.

[19] K. Chen, A. Harris, J. Draskovic, P. Schiffer, Granular fragility under thermal cycles, Granul. Matter 11 (May) (2009) 237–242.

[20] S. Plimpton, Fast parallel algorithms for short-range molecular dynamics, J. Computat. Phys. 117 (March) (1995) 1–19.

[21] M.L. Parks, S.J. Plimpton, R.B. Lehoucq, S.A. Silling, Peridynamics with LAMMPS: A User Guide, Technical Report, January, Sandia National Laboratories, Albuquerque, NM/Livermore, CA, 2008.

[22] H. Grubmuller, H. Heller, A. Windemuth, K. Schulten, Generalized Verlet algorithm for efficient molecular dynamics simulations with long-range interaction, Mol. Simulat. 6 (1991) 121–142.

[23] L. Silbert, D. Erta, G. Grest, T. Halsey, D. Levine, Geometry of frictionless and frictional sphere packings, Phys. Rev. E: Stat. Nonlin. Soft Matter Phys. 65 (February) (2002) 031304.

[24] Z. Zhou, A. Yu, P. Zulli, Particle scale study of heat transfer in packed and bubbling fluidized beds, AIChE J. 55 (April) (2009) 868–884.

[25] H. Zhang, Q. Zhou, H. Xing, H. Muhlhaus, A DEM study on the effective thermal conductivity of granular assemblies, Powder Technol. 205 (January) (2011) 172–183.

[26] J.T. Wu, Y.Q. Dai, Z.W. Wang, F.X. Liu, Study on the heat transfer in granular materials by DEM, Adv. Mater. Res. 233–235 (May) (2011) 2949–2954.

[27] W.L. Vargas, J.J. Mccarthy, Heat conduction in granular materials, AIChE J. 47 (5) (2001).

[28] J. Li, D. Mason, A computational investigation of transient heat transfer in pneumatic transport of granular particles, Powder Technol. 112 (October) (2000) 273–282.

[29] B. Chaudhuri, F.J. Muzzio, M.S. Tomassone, Modeling of heat transfer in granular flow in rotating vessels, Chem. Eng. Sci. 61 (October) (2006) 6348–6360.

[30] G. Batchelor, R. O'Brien, Thermal or electrical conduction through a granular material, Proc. R. Soc. Lond. A: Math. Phys. Sci. 355 (1682) (1977) 313–333.

[31] C. Kloss, C. Goniva, A. Hager, S. Amberger, S. Pirker, Models, algorithms and validation for opensource DEM and CFD-DEM, Prog. Comput. Fluid Dyn. 12 (2/3) (2012) 140–152.

[32] P.J. Gierszewski, Review of properties of lithium metatitanate, Fusion Eng. Des. 39–40 (September) (1998) 739–743.

[33] G. Piazza, J. Reimann, E. Günther, R. Knitter, N. Roux, J.D. Lulewicz, Characterisation of ceramic breeder materials for the helium cooled pebble bed blanket, J. Nucl. Mater. 307–311 (December) (2002) 811–816.